DOHERTY, R., BENSON, W. R., MAIENTHAL, M. & STEWART, J. McD. (1978). *J. Pharm. Sci.* **67**, 1698–1701.

GADRET, M., GOURSOLLE, M., LEGER, J. M. & COLLETER, J. C. (1975). *Acta Cryst.* B31, 1938–1942.

GADRET, M., GOURSOLLE, M., LEGER, J. M. & COLLETER, J. C. (1976). *Acta Cryst.* B32, 17–20.

GADRET, M., GOURSOLLE, M., LEGER, J. M., COLLETER, J. C. & CARPY, A. (1976). *Acta Cryst.* B32, 2757–2761.

HANSON, A. W. (1972). *Acta Cryst.* B28, 672–679.

HANSON, A. W. & BANNER, D. W. (1974). *Acta Cryst.* B30, 2486–2488.

HANSON, A. W. & RÖHRL, M. (1972). *Acta Cryst.* B28, 3567–3571.

JOHNSON, C. K. (1965). *ORTEP.* Report ORNL-3794. Oak Ridge National Laboratory, Tennessee, USA.

KARLE, I. L. & KARLE, J. (1981). *Proc. Natl Acad. Sci. USA,* **78**, 5938–5941.

KASHINO, S. & HAISA, M. (1983). *Acta Cryst.* C39, 310–312.

LAGUERRE, M., LEGER, J. M., MERLET, D., COLLETER, J. C. & DUBOST, J. P. (1982). *Acta Cryst.* B38, 2291–2293.

LEGER, J. M., GADRET, M. & CARPY, A. (1977). *Acta Cryst.* B33, 2156–2159.

MALAWSKA, B., GORCZYCA, M., CEBO, B. & KRUPIŃSKA, J. (1988). *Pol. J. Pharmacol. Pharm.* **40**, 173–181.

MALAWSKA, B., GORCZYCA, M., CHOJNACKA-WÓJCIK, E. & TARCZYŃSKA, E. (1982). *Pol. J. Pharmacol. Pharm.* **34**, 373–382.

MALAWSKA, B., GORCZYCA, M., FILIPEK, B., CROS, G. H., LIUTKUS, M. & SERRANO, J. J. (1990). 26ème Rencountres Internationales de Chimie Therapeutique, Montpellier.

MORGANROTH, J. (1985). *Drugs,* **29**(Suppl. 4), 14–20.

NARDELLI, M. (1983). *Comput. Chem.* **7**, 95–98.

OLEKSYN, B. J. (1987). *Crystal Chemistry of Cinchona Alkaloids and Related Compounds.* Uniw. Jagielloński, Rozprawy Habilitacyjne 135, Kraków, Poland.

PEETERS, O. M., BLATON, N. M., DE RANTER, C. J., DENISOFF, O. & MOLLE, L. (1980). *Cryst. Struct. Commun.* **9**, 851–856.

SCHWALBE, C. H. & SCOTT, D. K. (1979). *Br. J. Pharmacol.* **66**, 503 P.

SHELDRICK, G. M. (1976). *SHELX76.* Program for crystal structure determination. Univ. of Cambridge, England.

SHELDRICK, G. M. (1985). *SHELXS86. Crystallographic Computing* 3, edited by G. M. SHELDRICK, C. KRÜGER & R. GODDARD, pp. 175–189. Oxford Univ. Press.

SZEKERS, L. & PAPP, G. J. (1971). *Experimental Cardiac Arrhythmias and Antiarrhythmic Drugs.* Budapest: Akadémiai Kiadó.

YOO, C. S., ABOLA, E., WOOD, M. K., SAX, M. & PLETCHER, J. (1975). *Acta Cryst.* B31, 1354–1360.

Rotation Barriers in Crystals from Diffraction Studies: 2,2',4,4',6,6'-Hexa-*tert*-butylazobenzene

BY EMILY MAVERICK, KIRA MIRSKY, CAROLYN B. KNOBLER AND KENNETH N. TRUEBLOOD*

Department of Chemistry and Biochemistry, University of California, Los Angeles, California 90024, USA

AND L. ROSS C. BARCLAY

Chemistry Department, Mount Allison University, Sackville, New Brunswick, Canada E0A 3C0

Abstract

X-ray crystal studies yield similar anisotropic displacement parameters (ADPs) for the two chemically equivalent *para tert*-butyl groups in 2,2',4,4'.6.6'-hexa-*tert*-butylazobenzene ($C_{36}H_{58}N_2$) at 100 K. As the temperature rises, however, the ADPs increase more rapidly for one *para* group than for the other. Both *para* substituents have consistently larger libration amplitudes than those in the more crowded *ortho* positions. We have analyzed the ADPs with an internal-motion model which gives libration amplitudes for the *tert*-butyl groups at 100, 115, 128, 173, 200, 223 and 295 K. The results are consistent with rotational barriers for the six different groups of about 7 to more than 50 kJ mol^{-1}; at higher temperatures one of the *para* groups is best described by a twofold-disorder model. The low apparent barrier for this group and the disappearance of the disorder on cooling both suggest that the disorder is dynamic. Potential-energy calculations are employed to propose models for the hindering potential and for further disorder at room temperature. These calculations support the relative magnitudes of the barriers and the degree of disorder inferred from the X-ray diffraction data.

Introduction

For some time we have been studying internal motion in molecules in crystals, especially torsional oscillations, and have attempted to estimate barriers to such motion (Trueblood & Dunitz, 1983; Maverick & Dunitz, 1987). Molecules that contain chemically equivalent but crystallographically inequivalent groups that undergo internal motion are useful in testing the validity of such estimates. Studies over a range of temperatures can help to distinguish static disorder from motion of parts or all of

---

the molecule. Comparison of the barriers to such motion (which can be inferred from the amplitudes of the motion) with the results of packing-energy calculations should indicate whether the derived barriers are consistent, at least with presently used potential functions for interatomic interactions in crystals. If this approach is valid, it might be helpful in modifying such potentials.

To this end, we have reinvestigated at various temperatures from 100 to 295 K the structure of 2,2',4,4',6,6'-hexa-*tert*-butylazobenzene (1). In the solid state, the six *tert*-butyl groups are in six different environments, while in solution there is rapid motional averaging of the different environments even down to about 210 K, such that only the difference between the *ortho* and the *para* groups can be discerned (Barclay, Dust, Brownstein & Gabe, 1981). Thus this molecule offers an almost unique opportunity to study the motion of an internally librating group at once in chemically and crystallographically different environments and over a range of temperatures.

(1)
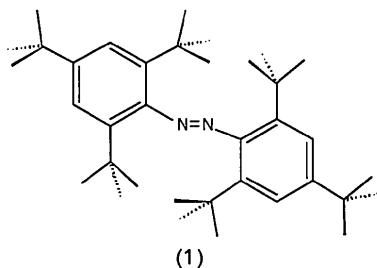
The crystal structure of (1) at 115 K was reported by Le Page, Gabe, Wang, Barclay & Holm (1980). The molecule has an approximate twofold axis; the two aromatic rings are distorted, and are twisted out of coplanarity (Fig. 1, dihedral angle 69°) to accommodate the crowded *ortho* substituents, so that these four chemically equivalent groups differ in their inter- and intramolecular close contacts. The two *para* substituents are more similar and less crowded within the molecule, yet are also in significantly different crystal environments. Le Page *et al.* (1980) reported that at room temperature the *para* groups are disordered; at 115 K they found that the disorder disappears. Even at 115 K, however, the anisotropic displacement parameters (ADPs) of the methyl C atoms in the *para* groups are larger than those in the *ortho* substituents, and those of the two *para* groups also differ appreciably from each other. This is evident on inspecting the published equivalent isotropic B values: the averages are 5·9 and 3·5 Å^2 for the *para* methyls, and 2·8, 2·8, 2·7 and 3·2 Å^2 for the *ortho* methyls, respectively.

We have studied the changes in the ADPs with temperature over the range 100 to 295 K, and have

analyzed the ADPs with a model for libration (Dunitz & White, 1973; Dunitz, Schomaker & Trueblood, 1988) that allows each of the six *tert*-butyl groups (attached rigid groups, ARGs) to move independently with respect to the aromatic system (MAIN) to which it is attached. We have tested a simple sinusoidal model (Trueblood & Dunitz, 1983) for the rotation of the *tert*-butyl groups over the entire temperature range and have also examined the consistency of the model with atom–atom potential calculations (Gavezzotti, 1985).

Data collection

The space group is *Pbca*, with one molecule of (1) in the asymmetric unit (see Table 1 for crystal data). Data were collected for one crystal at (in chronological order) 128, 173, 223 and 295 K, and for a second, somewhat larger, crystal at 295, 200 and 100 K. The 100 K data set was taken on a Huber diffractometer constructed by C. E. Strouse of this department; for all others a Picker FACS-1 instrument modified by Strouse was used. When we attempted to cool the second crystal to about 15 K, it split cleanly along the (001) face; we were unable to collect data below 100 K, although peaks were centered and scanned at several lower temperatures.

Refinement

The structure of Le Page *et al.* (1980) was confirmed with our 128 K data; thereafter, at each temperature, refinement was initiated with the starting coordinates from the 128 K analysis. All non-H atoms were numbered in the order given by Le Page *et al.* (1980). A modified version of *SHELX*76 (Sheldrick, 1976) was used for all full-matrix least-squares refinements, based on F, using reflections with $F_o > 3\sigma(F_o)$ and $1/\sigma^2$ weighting. Except for the disordered regions at
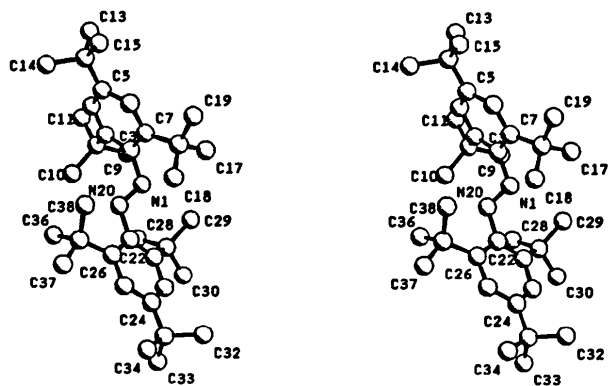

Fig. 1. Stereoview of (1) in the crystal, with the atomic numbering scheme; for clarity, the numbers of some ring atoms are omitted. No H atoms are shown.

Table 1. *Crystal data and refinement parameters*

Space group $Pbca$, $M_r = 518.84$, $F(000) = 2304$, $Z = 8$, $\mu = 0.30$ cm^{-1}; $0 < h < 19$, $0 < k < 20$, $0 < l < 27$, $0 < 2\theta < 50°$ ($h_{max} = 20$ for crystal 2, 295 K).

	Crystal 1 (0·50 × 0·25 × 0·30 mm)					Crystal 2 (0·50 × 0·50 × 0·30 mm)				
T (K)	128	173		223	295	100	200		295	
a (Å)	16·563(3)	16·632(3)		16·772(3)	16·802(5)	16·495(2)	16·639(4)		16·819(5)	
b (Å)	17·346(3)	17·330(3)		17·350(3)	17·307(4)	17·360(2)	17·290(4)		17·320(5)	
c (Å)	23·104(4)	23·150(4)		23·286(4)	23·302(6)	23·009(4)	23·176(5)		23·269(7)	
V (Å^3)	6638	6673		6776	6776	6589	6667		6678	
D_x (g cm^{-3})	1·038	1·033		1·017	1·017	1·046	1·034		1·017	
Measured reflections	6567	6512		7219	6588	11326	6498		6592	
Unique reflections[a]	5852	5890		5966	5969	5809	5885		5974	
R_{merge}					0·141	0·086				
$F > 3\sigma(F)$	2529	2368		2251	1989	4091	3129		2840	
Model[b]	1	1	2	2	2	1	1	2	2	3
Parameters refined	343	343	353	353	353	343	343	353	353	363
R	0·109	0·113	0·106	0·118	0·155	0·094	0·101	0·093	0·116	0·114
wR	0·091	0·094	0·088	0·094	0·122	0·096	0·094	0·085	0·100	0·098
S	1·78	1·88	1·76	1·88	2·24	2·85	1·97	1·80	2·04	2·01
Peaks[c]										
Maximum	0·37	0·36	0·45	0·36	0·41	0·36	0·53	0·26	0·30	0·33
Minimum	−0·36	−0·35	−0·32	−0·37	−0·36	−0·36	−0·33	−0·27	−0·28	−0·33
Occupancy	1·00	1·00	0·84[d]	0·74[d]	0·69[d]	1·00	1·00	0·86[d]	0·72[d]	0·72[d]/0·91[e]

Notes: (a) excluding space-group extinct reflections; (b) model 1 fully ordered, model 2 disorder at C13–C15, model 3 disorder at C13–C15 and at C32–C34; (c) peak heights in final difference map (e Å^{-3}); (d) occupancy of major conformer at C13–C15 (sum of major and minor occupancies = 1·00); (e) occupancy of major conformer at C32–C34 (sum of major and minor occupancies = 1·00).

higher temperatures (see below), all C and N atoms were refined with anisotropic displacement parameters. H atoms were refined as parts of rigid methyl groups, or riding (Sheldrick, 1976) on the attached aromatic C atom. The displacement parameters for H were fixed, and were adjusted in the last cycles to 0·01 Å^2 more than the equivalent isotropic U value for the attached C atom (C—H distance 1·08 Å).

Atomic scattering factors were taken from *International Tables for X-ray Crystallography* (1974, Vol. IV). All calculations were performed on DEC VAX 11/750, VAX 3100 and VAX 11/780 computers with the *UCLA Crystallographic Package* (1984) (including locally edited versions of *CARESS, PROFILE, ORTEP* and *SHELX*), a local molecular-geometry program (*MG*89), *THMA*11 (Dunitz et al., 1988) and *PLUTO*78 (Motherwell & Clegg, 1978).

With the first crystal, at 223 K, the final difference map showed significant peaks about midway between the methyl C atoms in one of the *para tert*-butyl groups, C12–C15, although no such peaks were evident at 128 or 173 K. Similar peaks were found, however, even at earlier stages in the refinement for the second crystal at 200 K (although not at 100 K), and for both crystals at room temperature. A disorder model, described as follows, was then used for C13, C14 and C15 for the 173, 200, 223 and 295 K data sets. Two groups of methyl C atoms, C13*A*–C15*A* and C13*B*–C15*B*, were kept nearly rigid by adding restraints (Sheldrick, 1976); bond distances to C12 were restrained to about 1·54 Å and C$_{Me}$···C$_{Me}$ distances within each group to about 2·50 Å. The relative occupancies were first refined, keeping isotropic displacement parameters (DPs) constant; thereafter the occupancies and the DPs for the 'minor' group were kept fixed, and

ADPs were refined for the 'major' group. H atoms for both conformers were placed in calculated positions after convergence. After thermal-motion analysis (see below) a similar disorder model was introduced for the other *para tert*-butyl group, C31–C34, at 295 K. Table 1 shows the effect of the disorder models (data at 173, 200 and 295 K) on the refinement parameters. The effect of introducing disorder at C32–C34 (at 295 K) is slight, but significant at the 0·005 confidence level (Hamilton, 1965).

Fig. 2 shows the thermal ellipsoids at 173 K, before a disorder model was introduced. The difference between the *para* groups at this temperature is evident.
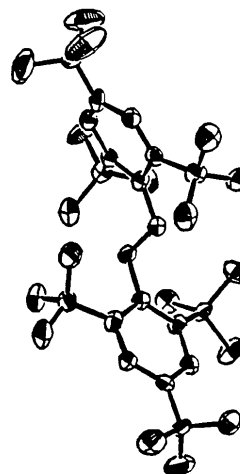
Fig. 2. View of (1) at 173 K. Orientation is the same as in Fig. 1. Thermal ellipsoids are drawn at the 50% probability level (Johnson, 1976).

Table 2. *Positional and displacement parameters for* C *and* N *atoms in* 2,2',4,4',6,6'-*hexa-tert-butylazobenzene at* 100 K

'Displacement parameters' are commonly called vibration parameters. Units of U_{ij} and isotropic U_{eq} are Å^2; units of each e.s.d., in parentheses, are those of the least significant digit of the corresponding parameter. Isotropic values are $1/(8\pi^2)$ times the 'equivalent B value' defined by Hamilton (1959). The anisotropic displacement parameter is defined as: $\exp[-2 \cdot 0\pi^2(U_{11}a^{*2}h^2 + U_{22}b^{*2}k^2 + U_{33}c^{*2}l^2 + 2 \cdot 0 U_{12}a^*b^*hk + 2 \cdot 0 U_{13}a^*c^*hl + 2 \cdot 0 U_{23}b^*c^*kl)]$. Positional and displacement parameters for H atoms are given in the supplementary material.

	x	y	z	U_{11}	U_{22}	U_{33}	U_{12}	U_{13}	U_{23}	U_{eq}
N1	0·4114 (3)	0·2403 (2)	0·1882 (1)	0·029 (3)	0·021 (2)	0·026 (2)	0·000 (2)	0·005 (2)	-0·001 (1)	0·025
C2	0·3771 (3)	0·2351 (2)	0·2465 (2)	0·024 (3)	0·022 (2)	0·025 (2)	-0·001 (2)	0·001 (3)	0·002 (2)	0·024
C3	0·3106 (3)	0·2775 (2)	0·2695 (2)	0·021 (3)	0·018 (2)	0·028 (2)	-0·002 (2)	-0·001 (2)	-0·004 (2)	0·022
C4	0·2725 (3)	0·2482 (2)	0·3185 (2)	0·024 (3)	0·023 (2)	0·029 (2)	0·002 (3)	0·003 (3)	-0·001 (2)	0·025
C5	0·2993 (3)	0·1803 (2)	0·3471 (2)	0·025 (3)	0·021 (2)	0·020 (2)	-0·002 (2)	-0·001 (2)	-0·003 (2)	0·022
C6	0·3708 (3)	0·1475 (2)	0·3268 (2)	0·023 (3)	0·020 (2)	0·026 (2)	-0·005 (2)	-0·005 (3)	0·003 (2)	0·023
C7	0·4123 (3)	0·1731 (2)	0·2782 (2)	0·025 (3)	0·021 (2)	0·027 (2)	-0·002 (2)	-0·007 (3)	-0·006 (2)	0·024
C8	0·2849 (3)	0·3599 (2)	0·2490 (2)	0·025 (3)	0·020 (2)	0·027 (2)	0·002 (2)	0·001 (3)	0·005 (2)	0·024
C9	0·3623 (4)	0·4072 (2)	0·2378 (2)	0·031 (3)	0·020 (2)	0·032 (2)	-0·005 (3)	-0·001 (3)	-0·001 (2)	0·027
C10	0·2284 (3)	0·3586 (2)	0·1952 (2)	0·028 (3)	0·022 (2)	0·034 (2)	-0·005 (2)	-0·004 (3)	0·003 (2)	0·028
C11	0·2391 (4)	0·4025 (2)	0·2972 (2)	0·045 (4)	0·024 (2)	0·047 (3)	0·005 (3)	0·013 (3)	0·005 (2)	0·039
C12	0·2542 (3)	0·1503 (2)	0·4004 (2)	0·028 (3)	0·023 (2)	0·025 (2)	-0·002 (3)	0·000 (3)	-0·001 (2)	0·025
C13	0·2576 (4)	0·2115 (3)	0·4487 (2)	0·052 (4)	0·037 (3)	0·027 (2)	-0·008 (3)	0·002 (3)	-0·005 (2)	0·038
C14	0·1647 (4)	0·1354 (3)	0·3845 (2)	0·034 (4)	0·036 (3)	0·029 (3)	-0·003 (3)	-0·002 (3)	0·005 (2)	0·033
C15	0·2904 (4)	0·0754 (3)	0·4243 (2)	0·042 (4)	0·036 (3)	0·033 (3)	0·004 (3)	-0·002 (3)	0·010 (2)	0·037
C16	0·4949 (3)	0·1357 (2)	0·2631 (2)	0·029 (3)	0·021 (2)	0·024 (2)	0·002 (2)	0·003 (3)	0·000 (2)	0·024
C17	0·5611 (3)	0·1975 (2)	0·2557 (2)	0·021 (3)	0·026 (2)	0·036 (3)	0·000 (2)	0·000 (3)	-0·005 (2)	0·028
C18	0·4892 (4)	0·0847 (2)	0·2083 (2)	0·026 (3)	0·031 (2)	0·034 (3)	0·004 (3)	0·000 (3)	-0·006 (2)	0·030
C19	0·5242 (3)	0·0833 (2)	0·3131 (2)	0·023 (3)	0·026 (2)	0·046 (3)	0·005 (3)	-0·002 (3)	0·006 (2)	0·032
N20	0·3589 (3)	0·2438 (2)	0·1485 (1)	0·023 (2)	0·023 (2)	0·022 (2)	0·001 (2)	-0·005 (2)	-0·002 (1)	0·023
C21	0·3916 (3)	0·2257 (2)	0·0911 (2)	0·023 (3)	0·021 (2)	0·024 (2)	0·004 (2)	-0·002 (2)	-0·003 (2)	0·022
C22	0·4540 (3)	0·2655 (2)	0·0613 (2)	0·019 (3)	0·024 (2)	0·022 (2)	-0·001 (2)	0·001 (2)	0·002 (2)	0·022
C23	0·4855 (3)	0·2301 (2)	0·0112 (2)	0·020 (3)	0·023 (2)	0·025 (2)	0·000 (2)	-0·001 (2)	0·001 (2)	0·023
C24	0·4564 (3)	0·1605 (2)	-0·0105 (2)	0·026 (3)	0·019 (2)	0·028 (2)	0·005 (2)	0·002 (3)	0·006 (2)	0·025
C25	0·3885 (3)	0·1280 (2)	0·0168 (2)	0·018 (3)	0·019 (2)	0·030 (2)	-0·002 (2)	0·001 (2)	-0·003 (2)	0·022
C26	0·3534 (3)	0·1600 (2)	0·0668 (2)	0·022 (3)	0·019 (2)	0·026 (2)	-0·001 (2)	-0·006 (3)	0·005 (2)	0·022
C27	0·4826 (3)	0·3489 (2)	0·0755 (2)	0·022 (3)	0·020 (2)	0·028 (2)	0·000 (2)	0·000 (3)	0·000 (2)	0·023
C28	0·4063 (3)	0·4001 (2)	0·0844 (2)	0·029 (3)	0·020 (2)	0·033 (2)	0·004 (3)	-0·003 (3)	-0·003 (2)	0·027
C29	0·5385 (3)	0·3516 (2)	0·1285 (2)	0·027 (3)	0·022 (2)	0·034 (2)	0·000 (3)	0·000 (3)	-0·006 (2)	0·028
C30	0·5295 (4)	0·3850 (2)	0·0245 (2)	0·038 (4)	0·026 (2)	0·038 (3)	-0·006 (3)	0·002 (3)	-0·001 (2)	0·034
C31	0·4939 (3)	0·1259 (2)	-0·0652 (2)	0·032 (3)	0·022 (2)	0·021 (2)	0·004 (3)	0·000 (3)	-0·002 (2)	0·025
C32	0·5857 (4)	0·1140 (3)	-0·0561 (2)	0·025 (3)	0·033 (2)	0·030 (3)	0·002 (3)	0·002 (3)	-0·006 (2)	0·029
C33	0·4813 (4)	0·1820 (2)	-0·1166 (2)	0·050 (4)	0·030 (2)	0·024 (2)	0·010 (3)	0·003 (3)	0·002 (2)	0·035
C34	0·4559 (4)	0·0476 (2)	-0·0822 (2)	0·033 (4)	0·024 (2)	0·040 (3)	-0·005 (3)	0·007 (3)	-0·008 (2)	0·033
C35	0·2734 (3)	0·1248 (2)	0·0900 (2)	0·022 (3)	0·022 (2)	0·036 (3)	0·001 (3)	0·001 (3)	0·002 (2)	0·027
C36	0·2063 (3)	0·1868 (2)	0·0915 (2)	0·023 (3)	0·028 (2)	0·040 (3)	-0·003 (3)	0·000 (3)	0·001 (2)	0·030
C37	0·2435 (4)	0·0595 (2)	0·0510 (2)	0·025 (3)	0·034 (2)	0·041 (3)	-0·003 (3)	-0·002 (3)	-0·003 (2)	0·034
C38	0·2833 (4)	0·0897 (2)	0·1512 (2)	0·030 (3)	0·033 (2)	0·034 (2)	-0·005 (3)	-0·007 (3)	0·008 (2)	0·032

Results

Final coordinates and ADPs for C and N atoms at 100 K are given in Table 2.* The standard deviations in positional parameters are of the order of 0·006 Å; even at 100 K, the e.s.d.'s of U_{ij} are large, typically about 10% of U_{ii}. Examination of the cell parameters (Table 1 and a plot with the supplementary material) shows that a and c increase with increasing temperature while b decreases slightly. Because two different crystals were used, and because for each cell axis the largest discrepancies are at 200 or 223 K, where the other evidence is that the conformational disorder is increasing rapidly (perhaps dependent on the rate or direction of temperature change), we

* Tables of atomic positions, displacement parameters, intramolecular distances, angles and torsion angles, observed and calculated structure factors with e.s.d.'s for the stuctures from crystal 2 at 100, 200 and 295 K, and differences in mean-square displacement amplitudes, calculated potential-energy curves, graphs of cell parameters *versus* T, and a packing diagram have been deposited with the British Library Document Supply Centre as Supplementary Publication No. SUP 53591 (119 pp.). Copies may be obtained through The Technical Editor, International Union of Crystallography, 5 Abbey Square, Chester CH1 2HU, England.

believe that the e.s.d.'s of the cell dimensions are not valid estimates of the reproducibility of measurements that might be made on different crystal specimens. The greater number of observations available from crystal 2 leads to a greater nominal precision for the results with this crystal; even so, treatment of the disorder (at the higher temperatures) involves arbitrary choices of model. These are thus not highly accurate or precise structure analyses.

There is a general increase in ADPs as temperature rises, but most structural features remain the same at all temperatures. For example, one methyl C atom in each *para* substituent nearly eclipses a ring C atom, the internal angles in the rings are always larger at the unsubstituted aromatic C atoms, C4, C6, C23 and C25, than at the C atoms where substituents are attached, and the dihedral angle between the two aromatic rings is essentially independent of temperature.

Analysis of displacement parameters

As stated above, the apparent motions of the chemically equivalent *para* groups C13–C15 and C32–C34

differ markedly in the crystal. The shapes of the ellipsoids suggest a libration of the *tert*-butyl groups about the bonds that attach them to the aromatic rings, and the larger ellipsoids at C13–C15 indicate a greater degree of dynamic or static disorder in that region. The anisotropic displacement parameters were analyzed with our program *THMA*11. The rigid-bond test (Hirshfeld, 1976) indicates, especially at the higher temperatures, that the ADPs are of poor quality; differences in mean-square displacement amplitudes (ΔMSDAs) along bonded directions are sometimes considerably larger than σ(ADP).* [The mean σ(ADP) is about 0·0025 Å^2, while the r.m.s. ΔMSDA along bonded directions is 0·0049 Å^2, at 100 K.] A 7-ARG model, with libration about the N=N bond, shows very little motion of one ring with respect to the other (about 2 deg^2). The agreement of calculated with observed ADPs is better if the molecule is treated as two separate $C_{18}H_{29}N$ moieties, each consisting of a rigid aromatic ring with an N atom (MAIN), and three ARGs (the *para* and two *ortho* *tert*-butyl groups). Table 3 lists the resulting mean-square libration amplitudes $\langle\varphi^2\rangle$, for the six ARGs in the molecule, and the agreement index R for each analysis.

Looking first at $\langle\varphi^2\rangle$ values calculated from ADPs from the 'ordered' model refinement, we see that $\langle\varphi^2\rangle$ for the *tert*-butyl groups increases with temperature, except from 115 to 128 K and from 173 to 200 K. For refinements with a *given* crystal, however, *i.e.* 128, 173, 223 K, only C9–C11 appears anomalous, showing a small decrease between 173 and 223 K, which, however, is less than one e.s.d. These observations suggest that the degree of thermal or static disorder varies from crystal to crystal. When disorder is introduced, similar discontinuities are seen: $\langle\varphi^2\rangle$(C13–C15) is smaller at 223 K than at 200, 173 or 128 K. This is no doubt correlated with the major-conformer occupancy, 84% at 173 K and 74% at 223 K for crystal 1, and 86% at 200 K for crystal 2. Therefore the calculations and comparisons described in detail below are based on data from the second crystal, at 100, 200 and 295 K, for which somewhat better precision is expected.

Because of the size of the molecule, the *overall* librational amplitudes, given by the L tensor, are never large. Even when no *internal torsional motion* is allowed for, the largest mean-square amplitude about any principal axis of L at 295 K is smaller than 14 deg^2, and at 100 K less than 4 deg^2. When motion of the ARGs is included, the values of L become even smaller. The magnitude of L along the axis of any ARG at 100 K never exceeds about 5% of the mean-square amplitude of the internal motion,

and at 200 and 295 K, none exceeds 10%.* The effect of including the correlations of internal and overall motion is small: when the ARG amplitudes are calculated with the Dunitz–White (Dunitz & White, 1973) model, the *changes* in the mean-square ARG amplitudes (from those calculated with the correlations) are usually smaller than their e.s.d.'s, and for the larger amplitudes, appreciably smaller.

Fig. 3 is a plot of $\langle\varphi^2\rangle$ for the C13–C15 and C32–C34 (*para*) and C36–C38 (*ortho*) groups at several temperatures. (The other three *tert*-butyl groups, in more crowded *ortho* positions, have smaller $\langle\varphi^2\rangle$ at all temperatures.) Again, as in Fig. 2, it is evident that the *para* groups C13–C15 and C32–C34 are far from equivalent in the crystal. Table 3 shows, however, that the introduction of the disorder model† (C13*A*–C15*A* and C13*B*–C15*B*) results in ADPs for the major conformer that are comparable to those for C32–C34. At room temperature, the analysis is complicated by larger uncertainties (fewer observations, stronger correlations). Inspection of Fig. 3 and Table 3 suggests that a disorder model should be considered for C32–C34 as well, at the higher temperatures, although no significant peaks appear in the appropriate positions in the difference map, even at 295 K. Such a model was tried, after the calculations described below.

Atom–atom potential calculations

If barriers to librational motion are to be calculated from the ADP analysis, a potential function is needed. This potential function will have (at least) threefold symmetry for an idealized *tert*-butyl group whose threefold axis is coincident with the libration axis. When the *tert*-butyl group is attached to a planar aromatic ring whose two sides are equivalent, then the potential function will have sixfold symmetry. In an isolated molecule of (1), assumed to have a twofold axis (as implied by the view in Fig. 1), the *tert*-butyl groups occur in pairs related by the dyad axis; these pairs thus have the same intramolecular potential functions. In the actual molecule of (1) in the crystal, none of these circumstances holds exactly, even the environment of the *para* groups being different.

Analysis of the motion of *tert*-butyl groups in other structures with a simple sinusoidal potential

---

* The table of ΔMSDAs for crystal 2 at 100 K is included in the supplementary material.

* We have therefore assumed that the correlation term $2\langle\varphi\lambda''\rangle$, which is included with the $\langle\varphi^2\rangle$ term in the ARG analysis (Dunitz, Schomaker & Trueblood, 1988; Schomaker & Trueblood, 1990), is negligible, a result that has seemed justified when the determinable sum $(\langle\varphi^2\rangle + 2\langle\varphi\lambda''\rangle)$ is as large as it is here (especially for the *para* groups).

† The position of the minor conformer is related to that of the major conformer by a rotation of approximately 180° about the C5—C12 bond.

Table 3. *Mean-square libration amplitudes* $\langle \theta^2 \rangle$ *(deg²) from THMA*11

$R = [\Sigma w(\Delta U)^2/\Sigma wU_{\text{obs}}^2]^{1/2}$. A more meaningful residual, R_d, evaluated for the diagonal elements only, was uniformly lower by 20–30%. 'Whole' means for the entire molecule; 'Half' applies when the molecule is analyzed in two separate, similar parts (see text).

	C13–15	C32–34	C9–11	C17–19	C28–30	C36–38	R
No disorder							
100 K[a]	30 (5)	27 (5)	17 (4)	17 (4)	11 (4)	23 (4)	0·15 (Whole)
	27 (5)	25 (5)	12 (5)	9 (4)	8 (4)	14 (4)	0·13 (Half)
115 K[b]	123 (14)	21 (10)	17 (10)	19 (10)	6 (9)	28 (10)	0·26 (Half)
128 K[c]	91 (11)	38 (9)	26 (8)	10 (8)	11 (8)	29 (9)	0·19 (Half)
173 K[c]	276 (20)	56 (10)	36 (11)	23 (11)	21 (9)	39 (9)	0·18 (Half)
200 K[a]	244 (14)	70 (8)	30 (8)	23 (8)	20 (7)	44 (7)	0·12 (Half)
223 K[c]	406 (23)	127 (13)	31 (11)	35 (11)	29 (10)	60 (11)	0·16 (Half)
With disorder at C13–C15							
173 K[d]	80 (12)	66 (11)	37 (8)	27 (9)	26 (9)	39 (9)	0·16 (Half)
200 K[e]	86 (9)	75 (8)	31 (6)	30 (6)	22 (7)	41 (7)	0·11 (Half)
223 K[f]	52 (15)	136 (13)	37 (10)	39 (10)	26 (10)	57 (10)	0·17 (Half)
295 K[g]	93 (15)	206 (15)	42 (10)	62 (11)	31 (10)	90 (11)	0·13 (Half)
With disorder at C13–C15 and C32–C34							
295 K[h]	76 (15)	116 (11)	44 (10)	64 (11)	28 (8)	89 (9)	0·13 (Half)

Notes: (a) second crystal; (b) parameters from Le Page *et al.* (1980); (c) first crystal; (d) first crystal, 84% occupancy; (e) second crystal, 86% occupancy; (f) first crystal, 74% occupancy; (g) second crystal, 72% occupancy; (h) second crystal, 72% occupancy at C13–C15, 91% at C32–C34.

has given rough agreement with the barriers and force constants determined by other methods (Trueblood & Dunitz, 1983). With (1), however, it is not obvious whether the *para* groups should be governed by a threefold or a sixfold potential. In Fig. 4 the dependence of the barrier height on the mean-square libration amplitude and on the selection of the symmetry of the potential function is shown [for a more complete discussion, see Maverick & Dunitz (1987)]. For example, a $\langle \varphi^2 \rangle$ value of 30 deg² at 100 K corresponds to a barrier of about 7 kJ mol⁻¹ for a sixfold cosine function, and about 20 kJ mol⁻¹ for a threefold function.
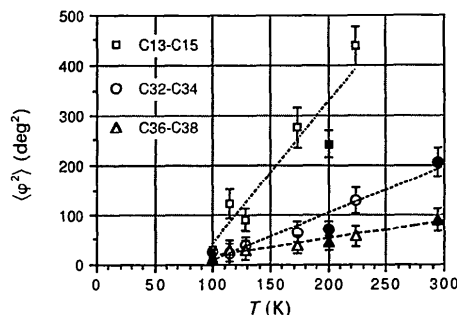
In the crystal, the molecules are arranged in layers perpendicular to *b*, with the long (*para–para'*) axis approximately parallel to *c*; as temperature rises, the increases in *a* and *c* permit *b* to decrease slightly (Table 1). The molecular environment in the crystal is illustrated in part in Fig. 5, where one can see that the surroundings of the *para* groups are different. More quantitative assessments of the packing,* and tests of the applicability of the idealized sinusoidal potentials described above, were made by calculating the non-bonded energy as a function of rotation angle of a rigid *tert*-butyl group turning in a static field (Gavezzotti, 1985). The crystal structures were

---

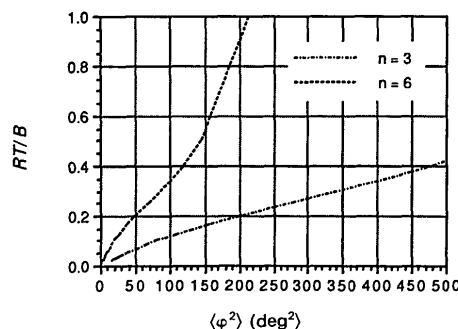* A packing diagram is included in the supplementary material.

Fig. 4. The relation between mean-square libration amplitude, $\langle \varphi^2 \rangle$, for threefold and sixfold cosine potentials and the dimensionless variable RT/B, with B the barrier height. For example, at 100 K, $RT = 831$ J mol⁻¹; $\langle \varphi^2 \rangle = 30$ deg² corresponds, for a sixfold potential, to a B value of about $8RT$, or nearly 7 kJ mol⁻¹, and, for a threefold potential, to about 20 kJ mol⁻¹. The values of $\langle \varphi^2 \rangle$ were calculated by Boltzmann averaging (Maverick & Dunitz, 1987); numerical integration was carried out by means of the Gauss approximation (Smith, 1986).

Fig. 3. Temperature dependence of the mean-square libration amplitude, $\langle \varphi^2 \rangle$, for the two *para* groups (C13–C15, C32–C34) and one of the *ortho* groups (C36–C38). The open symbols are for crystal 1 and the darkened symbols are for crystal 2. Values at 115 K were determined from ADPs in Supplementary Publication No. 35499. Error bars represent a range of ± 1 e.s.d. Dashed lines are least-squares fits to all the points for a given *tert*-butyl group; they are drawn to help the reader group the points and also because, as a first approximation, $\langle \varphi^2 \rangle$ is proportional to T at higher temperatures (Dunitz *et al.*, 1988).
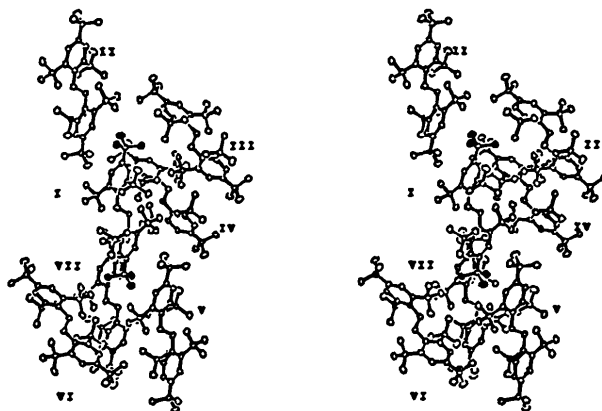
Fig. 5. The surroundings of the molecule in the crystal. In molecule (I), the orientation is similar to that in Figs. 1 and 2, with darkened ellipsoids for the C13–C15 (upper) and C32–C34 (lower) groups. The near neighbors shown are (II) $x, \frac{1}{2} - y, \frac{1}{2} + z$; (III) $x - \frac{1}{2}, y, \frac{1}{2} - z$; (IV) $\frac{1}{2} - x, y - \frac{1}{2}, z$; (V) $x, \frac{1}{2} - y, z - \frac{1}{2}$; (VI) $\frac{1}{2} + x, \frac{1}{2} - y, -z$; and (VII) $1 - x, -y, -z$ [behind molecule (I)].

analyzed as follows: all molecules within a 7·00 Å radius of the asymmetric unit were included; all non-bonded interactions within a 7·00 Å radius (except those *within* the rotating rigid group) were included. Positions from the X-ray studies of the second crystal at 100, 200 and 295 K were used without modification (with a few exceptions noted below), with the appropriate cell parameters. At the two higher temperatures, the 'crystal' was a cluster of major conformers.

Fig. 6* shows the calculated potential† for a complete rotation for each of the two *para* groups at 100 K. Near the observed positions (rotation angle zero), the curves for the two groups are quite similar. The maxima are doubtless too high, since no readjustment of atomic positions, either in the rotating group or in adjacent molecules, was allowed. Rotations of the *ortho* groups (not illustrated) are quite different from those of the *para* groups in symmetry and in energy: C17–C19 and C36–C38 show approximate threefold symmetry and maxima of more than 50 kJ mol⁻¹, while C9–C11 and C28–C30 give a threefold pattern (with slight dips near 60, 180 and −60°), and maximum energies more than 100 kJ mol⁻¹ above the minimum. Thus, unrealistic as the barrier heights may be, the calcula-

---

* Individual inter- and intramolecular curves are included in the supplementary material.

† The precision of the calculated energy was estimated to be of the order of 1–2 kJ mol⁻¹. This estimate was made in several ways, by recalculating the energy after: (*a*) altering three or four atomic positions by the amount of the e.s.d. from the X-ray analysis (Table 2); (*b*) at 100 K by using idealized H positions calculated from the final C and N coordinates in place of H positions obtained from rigid-group refinement; and (*c*) at 200 K by comparing the molecule from the no-disorder refinement with two disorder models, one with fixed C⋯C distances in the rigid groups of 2·50 Å, the other with distances of 2·48 Å. The maximum deviation in the energy near the minimum was about 2 kJ mol⁻¹. Rotation of a methyl group within a (fixed) *para* *tert*-butyl group alters the energy near the minimum by as much as 1·8 kJ mol⁻¹.

Table 4. *Difference in non-bonded energy* (kJ mol⁻¹) *between conformers* (*rotated by approximately* 180°) *as a function of temperature* (K)

Intramolecular non-bonded interactions plus intermolecular interactions give the total non-bonded energy.

| | C13–C15 | | | C32–C34 | | | |
| | Potential-energy calculations | | From | Potential-energy calculations | | From | |
	Intra	Inter	Total	occupancy[a]	Intra	Inter	Total	occupancy[a]
100 K	2	5	7		4	11	15	
200 K[b]	0	2	2	3	2	8	10	
295 K[c]	0	1	1	2	4	5	9	6

Notes: (*a*) method of calculation used was %minor/%major = exp(−ΔE/RT); (*b*) after refinement with disorder at C13–C15; (*c*) after refinement with disorder model for both groups.

tions indicate that the *para* groups can rotate much more freely than the *ortho* substituents, which follow a threefold potential, with the barriers for C36–C38 and C17–C19 lower than those for C28–C30 and C9–C11.

The potential for the *para* groups (Fig. 6) deviates somewhat from threefold symmetry because the three C_{Ar}—C_{tert}—C_{Me} angles are not identical: the angle for the methyl group that eclipses the aromatic carbon in the conformation found in the crystal is 113°, while the other two are 110°. (This is true for each of these two groups, essentially independent of temperature.) Consequently, when the *tert*-butyl group is rotated 120 or −120°, *with no change allowed* in the C_{Ar}—C_{tert}—C_{Me} angles, the calculated energy is higher because the eclipsing methyl is closer to the atoms of the aromatic core. When these bond angles are adjusted as the rotation proceeds, a situation presumably much closer to what actually occurs in the crystal, the threefold-related energy minima are more nearly equal (within about 2 kJ). Near −180° (see Fig. 6; the actual calculated minimum is at about −165°), where again the larger C_{Ar}—C_{tert}—C_{Me} angle is in an eclipsing position, the non-bonded
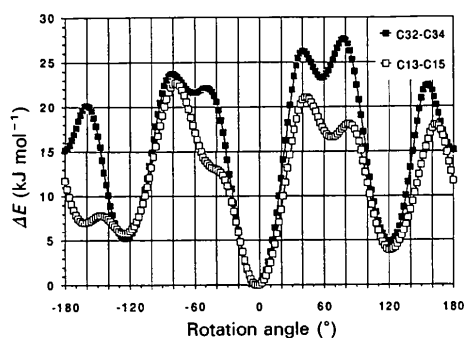

Fig. 6. Difference in non-bonded energy, the sum of intra- and intermolecular components, for the two *para* *tert*-butyl groups (at 100 K) as a function of rotation from the position found in the crystal (0°). The crystal environment is static for this calculation.
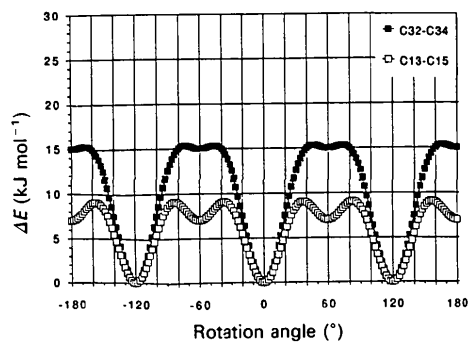

Fig. 7. An idealized potential function for rotation of the *para* *tert*-butyl groups, constructed from cosine functions with threefold and sixfold symmetry. The approximate barrier heights (and resulting well width near the minimum) come from ADP analysis, and the energy differences between conformers from the potential-energy calculations.

Table 5. *Rotation of tert-butyl groups: calculated barriers* (kJ mol^{-1})

Barriers are estimated from mean-square libration amplitudes (see Fig. 4 and Table 3).

	C13–C15		C32–C34		C9–C11	C17–C19	C28–C30	C36–C38
Sym[a]	6	3	6	3	3	3	3	3
100 K	7	23	7	25	60	86	101	50
115 K[b]	2	7	9	37	46	40	179	27
128 K	3	10	6	20	32	97	86	29
173 K	5[c]	14	7	20	31	50	55	29
200 K	6[c]	16	6	18	42	44	60	32
223 K	9[c]	28	4	12	39	37	56	26
295 K	9[c]	26	7[c]	18[c]	44	31	69	23
Error[d]	(1)	(4)	(1)	(2)	(10)	(10)	(20)	(4)

Notes: (a) 6 assumes a sixfold sinusoidal potential, 3 assumes a threefold sinusoidal potential; (b) using ADPs from Supplementary Publication No. 35499; (c) major conformer, see text; (d) representative propagated errors are shown for the 295 K analysis. Note that the higher barriers are very imprecise, because they correspond to small values of the libration amplitudes; see Table 3. The highest barriers may have errors of 50% or more.

energy for C13–C15 is only about 7 kJ mol^{-1} higher than at 0°, while the corresponding difference for C32–C34 is more than twice as large. (The sixfold subminima near ±60° are also lower for C13–C15 than for C32–C34, and are nearly equal in energy to those at about −180° if the bond angles at C$_{tert}$ are adjusted.) The differences near −180° are chiefly due to *inter*molecular interactions (Table 4). Thus, these energy calculations suggest that the net effective field 'felt' by the librating *tert*-butyl group has six wells, three (0, +120, −120°) with the energy of the observed structure and three (−180, −60, +60°) corresponding to the other conformer with an energy approximately 7 kJ mol^{-1} higher for C13–C15, and 15 kJ mol^{-1} higher for C32–C34. Fig. 7 shows such a potential; the wells have approximately the same width near the minimum as those in Fig. 6.

As the temperature rises, the calculated energy difference between conformers at the *para* positions decreases. For example, the energy at 200 K of the minor conformer C13B–C15B in a cluster of major conformers, whether its coordinates are obtained from the X-ray analysis or by calculated rotation in a cluster of major conformers, is only about 2 kJ mol^{-1} higher than that of the pure 'major' form. [Note that, under the rotation we are discussing, at 200 and 295 K the *only* (refined) differences between the three methyl groups, C13, C14, and C15, are the C$_{Ar}$—C$_{tert}$—C$_{Me}$ angles and the C$_{Ar}$—C$_{Ar}$—C$_{tert}$—C$_{Me}$ torsion angles, since the C$_{Me}$—C$_{tert}$—C$_{Me}$ distances and angles were fixed, and H positions were calculated after convergence.]

The differences in the minima alluded to in Fig. 7 are summarized in Table 4. They are consistent with an ordered structure at 100 K and the presence at 200 K of the higher-energy conformer in appreciable amounts for C13–C15, but not for C32–C34.

At room temperature, however, a significant proportion of the minor conformer at C32–C34 may be present. We therefore included C32B–C34B (as described above for C13–C15 under *Refinement*) in the X-ray analysis of the room-temperature data for crystal 2. The results were slightly better after intro-

duction of the disorder (see Table 1), and the ADPs of the major conformer gave a much lower $\langle\varphi^2\rangle$ value for C32A–C34A, nearer to $\langle\varphi^2\rangle$ of C13A–C15A (Table 3).

An additional check on the potential-energy calculations is provided by the relative occupancies of the two conformers at a given temperature. Energy differences calculated from the occupancies are given in Table 4 for 200 and 295 K. For C13–C15 they are not significantly different from those resulting from packing-energy calculations; for C32–C34, the occupancies suggest a slightly, but hardly significantly, lower energy difference.

Concluding remarks

Barrier heights hindering rotation of the *tert*-butyl groups in (1), estimated from ADP analysis, are shown in Table 5. Data from both crystal 1 and crystal 2 have been included. The barriers assuming a threefold potential are higher for *ortho* than for *para* substituents, and are lower for C36–C38 than for the other *ortho* groups. This agrees with the trend suggested by the potential-energy calculations discussed above, except for C17–C19, which according to the calculations should behave like C36–C38. The ADP analysis does not distinguish clearly between the *para* groups at 100 K, nor at higher temperatures *after disorder has been introduced*. The difference between them may be explained if the rotation is governed by a potential like that in Fig. 7, such that a methyl C atom may nearly eclipse *either* of the neighboring unsubstituted ring C atoms. Calculations indicate that the two conformations have approximately the same *intra*molecular energy, but that the packing favors one conformer at each *para* position. As the temperature rises, the conformers at C13–C15 become nearly equal in energy and the barrier is low enough (about 7–9 kJ mol^{-1}) that a sizeable proportion of the higher-energy conformer may be present, even at temperatures as low as 200 K. At C32–C34, however, one conformer is still highly favored even at 295 K, suggesting that at lower temperatures the

potential has effective threefold symmetry, with a barrier near 20 kJ mol^{-1}.

To be sure, the poor quality of the ADPs in these structures limits the precision of the barrier heights calculated from them, and the arbitrary choices in disorder-model refinement limit the precision of the energy differences calculated from non-bonded potentials. Nevertheless we are encouraged by the complementary and consistent results from potential-energy calculations and from ADP analysis to continue looking at crystal structures containing librating, possibly rigid groups that are chemically but not crystallographically equivalent. We plan to study (1) and related molecules using low-temperature solid-state ^{13}C NMR, and plan also to make variable-temperature crystal structure analyses of other compounds with tert-butyl and similar substituents.

References

BARCLAY, L. R. C., DUST, J. M., BROWNSTEIN, S. & GABE, E. J. (1981). Org. Magn. Reson. **17**, 175–177.
DUNITZ, J. D., SCHOMAKER, V. & TRUEBLOOD, K. N. (1988). J. Phys. Chem. **92**, 856–867.
DUNITZ, J. D. & WHITE, D. N. J. (1973). Acta Cryst. A**29**, 93–94.
GAVEZZOTTI, A. (1985). J. Am. Chem. Soc. **107**, 962–967.
HAMILTON, W. C. (1959). Acta Cryst. **12**, 609–610.
HAMILTON, W. C. (1965). Acta Cryst. **18**, 502–510.
HIRSHFELD, F. L. (1976). Acta Cryst. A**32**, 239–244.
JOHNSON, C. K. (1976). ORTEPII. Report ORNL-5138. Oak Ridge National Laboratory, Tennessee, USA.
LE PAGE, Y., GABE, E. J., WANG, Y., BARCLAY, L. R. C. & HOLM, H. L. (1980). Acta Cryst. B**36**, 2846–2848.
MAVERICK, E. & DUNITZ, J. D. (1987). Mol. Phys. **62**, 451–459.
MOTHERWELL, W. D. S. & CLEGG, W. (1978). PLUTO78. Program for plotting crystal and molecular structures. Univ. of Cambridge, England.
SCHOMAKER, V. & TRUEBLOOD, K. N. (1990). To be published.
SHELDRICK, G. M. (1976). SHELX76. Program for crystal structure determination. Univ. of Cambridge, England.
SMITH, D. M. (1986). Byte, (December), pp. 113–122.
TRUEBLOOD, K. N. & DUNITZ, J. D. (1983). Acta Cryst. B**39**, 120–133.
UCLA Crystallographic Package (1984). Univ. of California, Los Angeles, USA.

X-ray Powder Diffraction Studies of Alkanes: Unit-Cell Parameters of the Homologous Series C₁₈H₃₈ to C₂₈H₅₈

BY A. R. GERSON, K. J. ROBERTS* AND J. N. SHERWOOD

Department of Pure and Applied Chemistry, University of Strathclyde, Glasgow G1 1XL, Scotland

Abstract

Synchrotron radiation high-resolution powder diffraction has been applied to determination of the unit-cell parameters of n-alkanes in the range $C_{18}H_{38}$ to $C_{28}H_{58}$. The data confirm the previously reported results for $C_{18}H_{38}$, $C_{20}H_{42}$, $C_{23}H_{48}$ and $C_{25}H_{52}$. With the exception of $C_{24}H_{50}$ and $C_{26}H_{54}$, these data support the predictions made for the other homologues in this series by Nyburg & Potworowski [Acta Cryst. (1973), B**29**, 349–352] i.e. $C_{18}H_{38}$, $C_{20}H_{42}$ and $C_{22}H_{46}$ – triclinic unit cells ($Z = 1$), $C_{28}H_{58}$ – monoclinic unit cell ($Z = 2$), and $C_{19}H_{40}$, $C_{21}H_{44}$, $C_{23}H_{48}$, $C_{25}H_{52}$ and $C_{27}H_{56}$ – orthorhombic unit cells ($Z = 4$). In contrast, $C_{24}H_{50}$ and $C_{26}H_{54}$ are found to have lattice parameters consistent with a triclinic (pseudo-monoclinic) unit cell containing two molecules possibly arranged in a polytypic conformation of two

triclinic ($Z = 1$) unit cells related by a pseudo-twofold axis.

1. Introduction

The structures of n-alkanes (C_nH_{2n+2}) in the range $10 < n < 36$ are of fundamental and technological importance. The first structural studies on the n-alkanes are probably due to Müller (1928, 1930, 1932). Lattice parameters have been measured for $C_{18}H_{38}$ (Müller & Lonsdale, 1948), $C_{20}H_{42}$ (Crissman, Passaglia, Eby & Colson, 1970), $C_{23}H_{46}$ (Retief, Engel & Boonstra, 1985a,b) and $C_{25}H_{52}$ (Retief et al., 1985a,b). Full structures have been determined for $C_{18}H_{38}$ ($Z = 1$, $P\bar{1}$) (Nyburg & Lüth, 1972) and for the monoclinic ($Z = 2$, $P2_1/a$) (Schearer & Vand, 1956) and orthorhombic ($Z = 4$, $Pca2_1$) (Teare, 1959) polymorphs of $C_{36}H_{74}$. These three structures are shown schematically in Fig. 1. Nyburg & Potworowski (1973) predicted the lattice parameters of n-alkanes in the range $n = 6$–40.

* Also at SERC Daresbury Laboratory, Warrington, WA4 4AD, England.